BUTTERWORTH HEINEMANN

Free convection heat transfer in multiple vertical channels

J. M. Floryan and M. Novak
Department of Mechanical Engineering, The University of Western Ontario, London, Ontario, Canada

Free convection heat transfer in multiple parallel vertical channels with isothermal walls is considered in this paper. Systems consisting of two, three and an infinite number of channels located side by side and with aspect ratios (the ratio of channel height to its width) ranging from 5 to 20 and for Grashof numbers, based on the channel width, up to 10^5 were investigated numerically. Results show that the heat transfer in a channel is affected by its interaction with the neighboring channels. This interaction depends upon the number of participating channels; it increases with an increase of the Grashof number and decreases with an increase of the distance between the channels. Compared with a single isolated channel, the Nusselt number in the case of a two-channel system increases by up to 5% on the channel inner wall (wall closer to the other channel) and decreases by up to 5% on the channel outer wall. When an infinite number of channels is present (periodic configuration), the Nusselt number increases by up to 18%. When heat transfer only in the entrance region of the channel is considered (the first 10% of the channel total length), the interaction between the channels increases the corresponding Nusselt number by up to 38% on the channel inner wall and decreases it by up to 33% on the channel outer wall for a two-channel system and increases it by up to 48% for the periodic configuration. Correlations permitting quick determination of the Nusselt numbers for both configurations are given.

Keywords: free convection; multiple vertical channels

Introduction

Among various methods of cooling of electronic devices, cooling by free convection has an obvious advantage because of its passive character. Even increasing cooling requirements necessitate, however, thorough evaluation of heat transfer characteristics in geometries found in electronic devices. Cooling of computer boards can be studied by idealizing them as forming vertical channels (see Figure 1). Heat transfer in such channels is the subject of this analysis.

Free convection heat transfer in a single isolated vertical channel with isothermal walls has attracted the interest of many investigators beginning with Elenbaas (1942). A recent review of this problem can be found in Naylor et al. (1991).

Numerical solutions of the Navier–Stokes and energy equations for this configuration based on various approximations were presented by Bodoia and Osterle (1962), Aung et al. (1972), Kettleborough (1972) and Nakamura et al. (1982). In 1991, Naylor et al. presented a full elliptic solution of the field equations. In their study, the Navier–Stokes and the energy equations were solved using novel boundary conditions given by Jeffrey–Hammel flow. Compared with the previous numerical works, these boundary conditions represent more truthfully the real fluid flow situation in the channel entrance regions. The solution, describing in detail the local Nusselt number distribution and other local quantities primarily at the channel entrance region, was given for the Grashof number range $50/8 \leq Gr \leq 5/8 \times 10^4$ and for the channel aspect ratios (the ratio of the channel length to its width) equal to 5, 8.5, and 12. The accuracy of the results was assessed by comparing them with the experimental data. Discussion of the other available numerical simulations based on the Navier–Stokes equations as well as on the simplified boundary layer equations for various inlet boundary conditions was given.

The existing analyses have focused on the case of a single isolated channel. Because, typically, several computer boards are installed next to each other, we must address the question of how the heat transfer in the channel is affected by the presence of other near-by channels. The objective of this work is determination of the heat transfer characteristics of a system of parallel (identical) vertical channels.

The heat transfer in a system of channels depends upon the number of channels involved. At one extreme, the system may consist of a single channel (simplest configuration, Figure 1), and its characteristics have already been extensively studied in the literature (see preceding discussion). At the opposite extreme, the system may consist of an infinite number of channels with each channel forming a periodic segment (see Figure 3). Performance of a system consisting of a finite number of channels is expected to fall somewhere between the above

Address reprint requests to Dr. J. M. Floryan, Department of Mechanical Engineering, The University of Western Ontario, London, ON, N6A 5B9, Canada.

Received 5 May 1994; accepted 9 December 1994

Int. J. Heat and Fluid Flow 16: 244–253, 1995

655 Avenue of the Americas, New York, NY 10010

0142-727X/95/$10.00
SSDI 0142-727X(94)0022-5

cases. When the number of channels in a system increases, the channels in the middle of the system are expected to perform as periodic channels, while those close to the edges of the system will have different heat transfer characteristics because of the presence of edge effects. In this study, we analyze in detail the performance of periodic channels (limiting configuration) and the performance of systems consisting of two (see Figure 2) and three channels (see Figure 16). These cases permit us to assess the performance of very large systems, including the extent, the character and the magnitude of the edge effects.

Martin et al. (1991) studied heat transfer in a periodic channel arrangement for a fully developed flow regime corresponding to low Grashof numbers. They considered infinitely thin walls and, thus, were unable to study the effect of variation of distance between the channels. They also have not studied the effect of variations of the channel aspect ratios. As shown later, the range of Grashof numbers they studied is not of particular importance for the problem of interest here.

Kim et al. (1991) studied a periodic channel arrangement with conducting walls of finite thickness. They assumed constant uniform velocity distribution at the channel inlet independent of distance between the channels and modeled flow field using parabolized Navier–Stokes and energy equations. Therefore, their model is unable to capture the strong interaction phenomena taking place at channel inlet and the resulting higher induced flow rates.

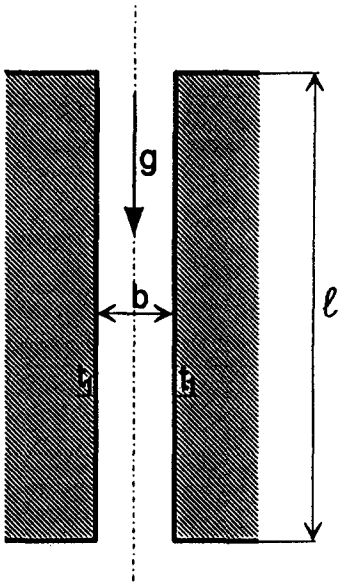

Figure 1 Single (isolated) vertical channel

Problem formulation

Three geometrical configurations subject to investigation are shown in Figures 1–3. The fluid is assumed to be well described by the Boussinesq approximation. The free convection heat transfer in the channels can be determined by solving the Navier–Stokes, continuity and energy equations in the following form:

$$\frac{\partial U}{\partial X}+\frac{\partial V}{\partial Y}=0 \tag{1}$$

$$\mathrm{Gr}^{1/2}\left(U\frac{\partial U}{\partial X}+V\frac{\partial U}{\partial Y}\right)=\frac{\partial P}{\partial X}+\left(\frac{\partial^2 U}{\partial X^2}+\frac{\partial^2 U}{\partial Y^2}\right) \tag{2}$$

$$\mathrm{Gr}^{1/2}\left(U\frac{\partial V}{\partial X}+V\frac{\partial V}{\partial Y}\right)=-\frac{\partial P}{\partial Y}+\mathrm{Gr}^{1/2}T^*+\left(\frac{\partial^2 V}{\partial X^2}+\frac{\partial^2 V}{\partial Y^2}\right) \tag{3}$$

$$\mathrm{PrGr}^{1/2}\left(U\frac{\partial T^*}{\partial X}+V\frac{\partial T^*}{\partial Y}\right)=\left(\frac{\partial^2 T^*}{\partial X^2}+\frac{\partial^2 T^*}{\partial Y^2}\right) \tag{4}$$

Notation

$a(A)$	Dimensional (dimensionless) distance between channels (see Figures 2 and 3)
b	Channel width (see Figures 1–3)
Gr	Grashof number based on the channel width = $g\beta(t_1 - t_0)b^3/\nu^2$
$\tilde{\mathrm{Gr}}$	Modified Grashof number = $\mathrm{Gr}(b/\ell)$
g	Gravitational acceleration
h	Mean convection heat transfer coefficient
h_{loc}	Local convection heat transfer coefficient
k	Thermal conductivity of air
ℓ	Channel length (see Figures 1–3)
ℓ_b	Length of the inlet zone for periodic channel system (see Figure 3)
L	Dimensionless channel length [or channel aspect ratio (= ℓ/b)]
L_b	Dimensionless length of the inlet zone for periodic channel system
Nu	Mean Nusselt number based on the channel width = hb/k
Nu_{loc}	Local Nusselt number based on the channel width = $h_{loc}b/k$
P	Dimensionless pressure
P^*	Reference pressure
Pr	Prandtl number
$r(R)$	Dimensional (dimensionless) radial coordinate
$r_i(R_i)$	Dimensional (dimensionless) radius of the channel inlet zone for a two-channel system (see Figure 2)
t_1	Channel wall temperature
t_0	Ambient air temperature
T^*	Dimensionless temperature
U	Dimensionless horizontal velocity component
U^*	Reference velocity
V	Dimensionless vertical velocity component
V_r	Dimensionless radial velocity component
V_e	Dimensionless tangential velocity component
$x(X)$	Dimensional (dimensionless) horizontal coordinate
$y(Y)$	Dimensional (dimensionless) vertical coordinate

Greek

β	Volumetric thermal expansion coefficient
μ	Dynamic viscosity
ν	Kinematic viscosity
δ	Exponent defined by Equation 8

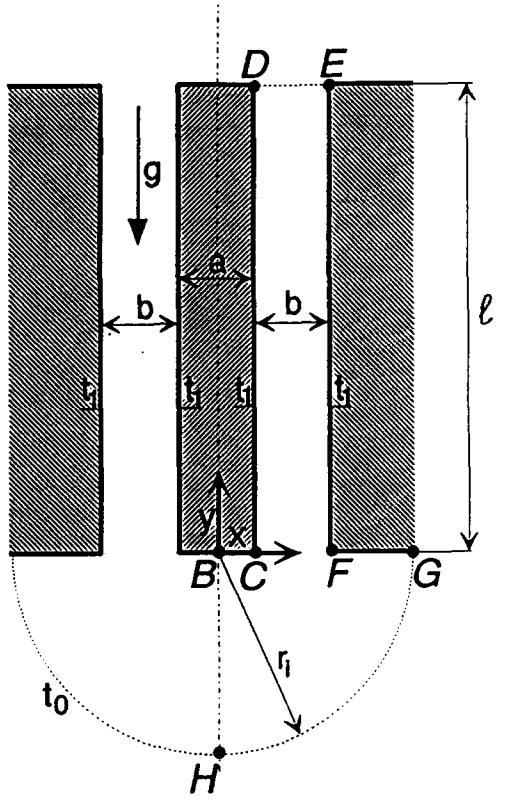

Figure 2 Two-channel system

All quantities in Equations 1–4 have been made dimensionless using the channel width b as a length scale, $U^* = \alpha \mathrm{PrGr}^{1/2}/b$ as a velocity scale, and $P^* = \mu U^*/b$ as a pressure scale. Here, α denotes the thermal diffusivity, and μ stands for the dynamic viscosity. The dimensionless temperature T^* was defined as $T^* = (t - t_0)/(t_1 - t_0)$, where t_1 denotes the temperature of the channel walls, t_0 is the ambient temperature, and t stands for the dimensional temperature. The Grashof number Gr is defined as $\mathrm{Gr} = g\beta b^3(t_1 - t_0)/\nu^2$, where g is the gravitational acceleration, β stands for the volumetric expansion coefficient, and ν denotes the kinematic viscosity. The Prandtl number Pr has the usual definition, $\mathrm{Pr} = \nu/\alpha$. These equations are subject to boundary conditions whose form is dictated by the geometry of the solution domain. These conditions are discussed on a case-by-case basis in the following sections.

The governing equations were solved numerically using FIDAP (Fluid Dynamics International, 1991) code. This code is based on the finite element discretization. Comparison of numerical simulations with experiments made by Naylor et al. (1991), Naylor and Tarasuk (1993a, b) and Straatman et al. (1993), demonstrate that the code faithfully reproduces the actual physics of the flow. Because of this, the present investigation is limited to computer simulations only.

Single isolated channel

The geometry of the flow domain is shown in Figure 1. The channel walls are assumed to be isothermal, while the bottom walls are assumed to be adiabatic. The relevant boundary conditions are described by Naylor et al. (1991). This configuration, which has been extensively studied in the literature, forms one of our limiting cases (i.e., single-channel system) and is included for comparison purposes. Results reproduced as a part of this study agree very well with the numerical and experimental data given by Naylor et al. (1991). For example, the comparison of numerical results for $\mathrm{Gr} = 80{,}000$, $L = 12$, and $\mathrm{Pr} = 0.7$ showed that the mean Nusselt number evaluated on a grid consisting of 13,141 nodes ($\mathrm{Nu} = 4.727$) does not differ from their results based on 10,333 grid ($\mathrm{Nu} = 4.690$) by more than 1% and from those based on 14,369 nodes ($\mathrm{Nu} = 4.714$) by more than 0.3%.

The reader may note that the present study also extends the range of the Grashof numbers considered by Naylor et al. (1991) by 60% ($\mathrm{Gr}_b \leq 5 \times 10^4$).

Two-channel system

Description of the flow geometry

We begin with the simplest multichannel system; i.e., a system consisting of just two channels, as sketched in Figure 2. Because of the symmetry, it is sufficient to consider only half of this system. The relevant boundary conditions have the following form (see Figure 2):

Line H–B:

$$U = \partial V/\partial X = \partial T^*/\partial X = 0 \quad \text{for} \quad X = 0, \quad -R_i \leq Y \leq 0$$

Line B–C:

$$U = V = \partial T^*/\partial Y = 0 \quad \text{for} \quad 0 \leq X < 0.5A, \quad Y = 0$$

Line C–D:

$$U = V = 0, \quad T^* = 1 \quad \text{for} \quad X = 0.5A, \quad 0 \leq Y \leq L$$

Line D–E:

$$\partial U/\partial Y = \partial V/\partial Y = \partial T^*/\partial Y = 0 \quad \text{for} \quad 0.5A \leq X < 0.5A + 0.5, \quad Y = L$$

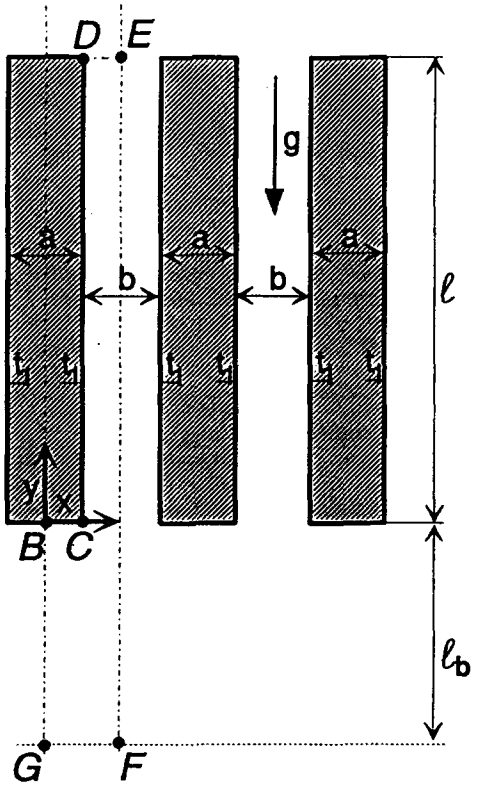

Figure 3 Infinite number of channels (periodic configuration)

Line E–F:

$$U = V = 0, \quad T^* = 1 \quad \text{for} \quad X = 0.5A + 1, \quad 0 \le Y \le L$$

Line F–G:

$$U = V = \partial T^*/\partial Y = 0 \quad \text{for} \quad 0.5A + 1 \le X \le R_i, \quad Y = 0$$

Semicircular boundary G–H:

$$V_6 = T^* = 0, \quad -P + \partial V_r/\partial R = 0$$

The preceding boundary conditions assume that the bottom walls are adiabatic, the vertical walls are isothermal, the first-order extrapolation approximation is employed at the exits from the channels (fully developed flow at the channel outlet), and the inflow field sufficiently far away from the inlets to the channels (R_i sufficiently large) is well approximated by the Jeffrey–Hammel flow. The distance R_i was determined through numerical experiments; i.e., calculations were repeated with sequentially increasing R_i until the inflow boundary conditions were located sufficiently far from the channels so that any further increase of R_i did not affect the flow and heat transfer characteristics in the channels. $R_i = 7$ was found to be sufficient for all calculations.

Local heat transfer at a channel wall is described in terms of the local Nusselt number, $\mathrm{Nu}_{\mathrm{loc}} = h_{\mathrm{loc}} b/k = \partial T^*/\partial X_{\mathrm{WALL}}$. The global heat transfer from the wall in each channel can be expressed in terms of the mean Nusselt number defined as follows:

$$\mathrm{Nu} = 1/L \int_0^L \mathrm{Nu}_{\mathrm{loc}} \, dY \tag{5}$$

The objective of this study is the determination of the mean Nusselt number Nu as a function of the Grashof number Gr, the channel length (or aspect ratio) L, and the distance between the channels A. To carry out the calculations, a grid of 3,525 nine-node quadrilateral elements (14,275 nodes) was used. Figure 4a depicts the grid structure at the channel inlet zone. To ensure the accuracy of the results, numerous tests with different grid densities were made. The results of testing for Gr = 80,000, Pr = 0.7, $L = 20$, and $A = 1$ are shown in Table 1.

It can be seen that in the case of the inlet zone radius $R_i = 7$, the change of grid density from 9,455 to 14,275 nodes does not affect the mean Nusselt number by more than 0.1% for both the inner and the outer walls. Further increase of the grid density from 14,275 to 16,405 nodes results in an even smaller change of the mean Nusselt number. For all three grids tested, the differences in the corresponding local Nusselt numbers were observed not to exceed 2% at the distance $Y \approx 1.5$ from the channel entrance and 1% near the channel exit. When the inlet zone radius was increased from $R_i = 7$ to $R_i = 8$, the resulting change of the mean Nusselt number was negligible (see Table 1). Based on these results a grid of 14,275 nodes and $R_i = 7$ was chosen for the majority of the calculations. A complimentary extrapolation study showed that the error of evaluation of the mean Nusselt numbers on this grid is no worse than 2%.

Results

Calculations showed that the flow pattern, especially in the channel entrance region, is strongly affected by the channel length, Grashof number, and the location of the neighboring channel. In longer channels with sufficiently high Grashof numbers, flow separation occurs in the channel entrance region, causing a substantial reduction of heat transfer in this area. For the same Grashof number and shorter channels, the separation is either much smaller or does not occur at all.

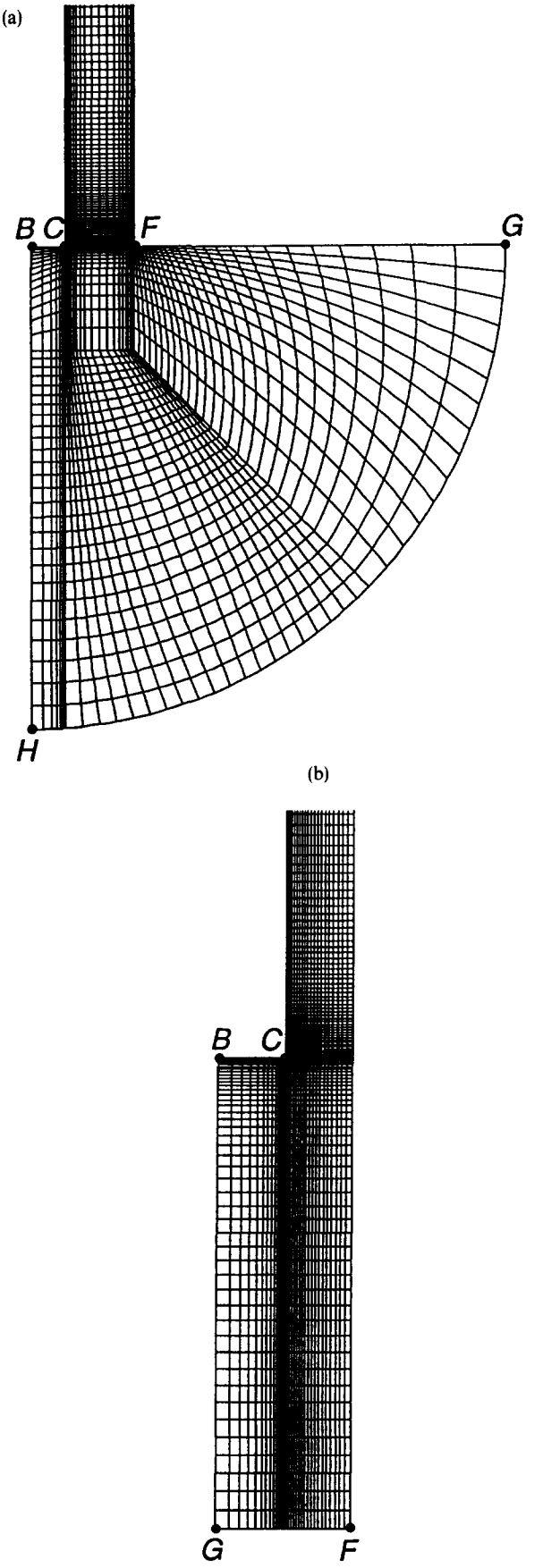

Figure 4 Finite element mesh structure in the entrance zone of a) a two-channel system and b) a periodic channel system

Table 1 Two-channel system; the mean Nusselt number

Radius inlet zone	Number grid points	Nu inner wall*	Nu outer wall†
$R_i = 7$	9,455	4.282	4.131
	14,275	4.286	4.135
	16,405	4.287	4.136
$R_i = 8$	14,773	4.285	4.135

* C–D in Figure 2
† E–F in Figure 2.

A typical flow pattern in a longer channel with high Grashof number $Gr = 10^5$, $R_i = 7$, $A = 2$, and $L = 12$ is shown in Figure 5. The distance between the channels is large and equal to twice the channel width. It can be seen that the flow distribution in each channel is affected by the presence of the neighboring channel; i.e., the velocities (and streamlines) along both the inner wall (wall closer to the other channel) and the outer wall (wall more distant from the other channel) are different.

Figure 6a gives a detailed picture of the flow separation pattern in the channel inlet zone. The fluid separates downstream from the entrance corners because of high induced velocity. Figure 6b depicts the flow pattern inside the channel entrance region for channels located very close to each other ($A = 0.1$) and with other parameters the same as those in Figure 6a. Comparison of Figures 6a and 6b shows that bringing the channels closer together decreases the separation on the inner wall but increases the separation on the outer wall. This is obviously caused by the change of the overall shape of the inlet zone and can be explained as follows. Because there is very little distance between channels, the flow near the leading edge of the inner wall enters the channel almost vertically, and the horizontal velocity component is insufficient to cause the separation. Fluid at the outer wall must turn around the corner, but it is not helped by the fluid turning in the opposite sense at the inner wall. Consequently, the separate region on the outer wall becomes much larger.

Figure 7 shows the grid density around the flow separation area. Even a very small separation area on the inner wall is covered roughly by 25 nodes, which guarantees sufficient resolution of the flow field.

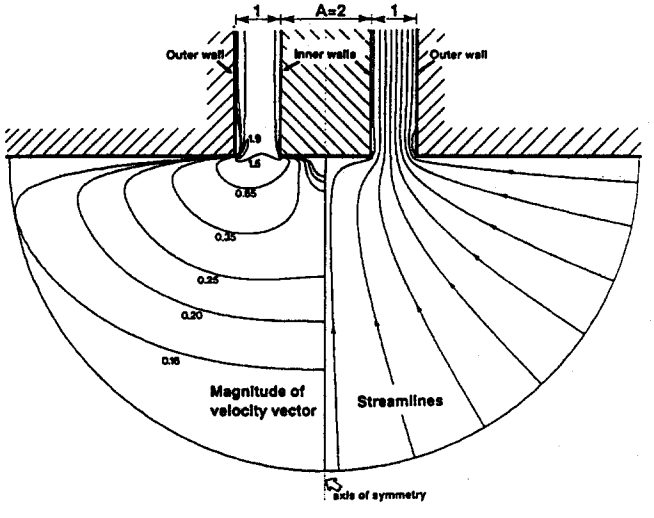

Figure 5 Two-channel system: Streamlines and magnitude of the velocity vector at the channel inlet zone: $Gr = 10^5$; $L = 12$; and $A = 2$

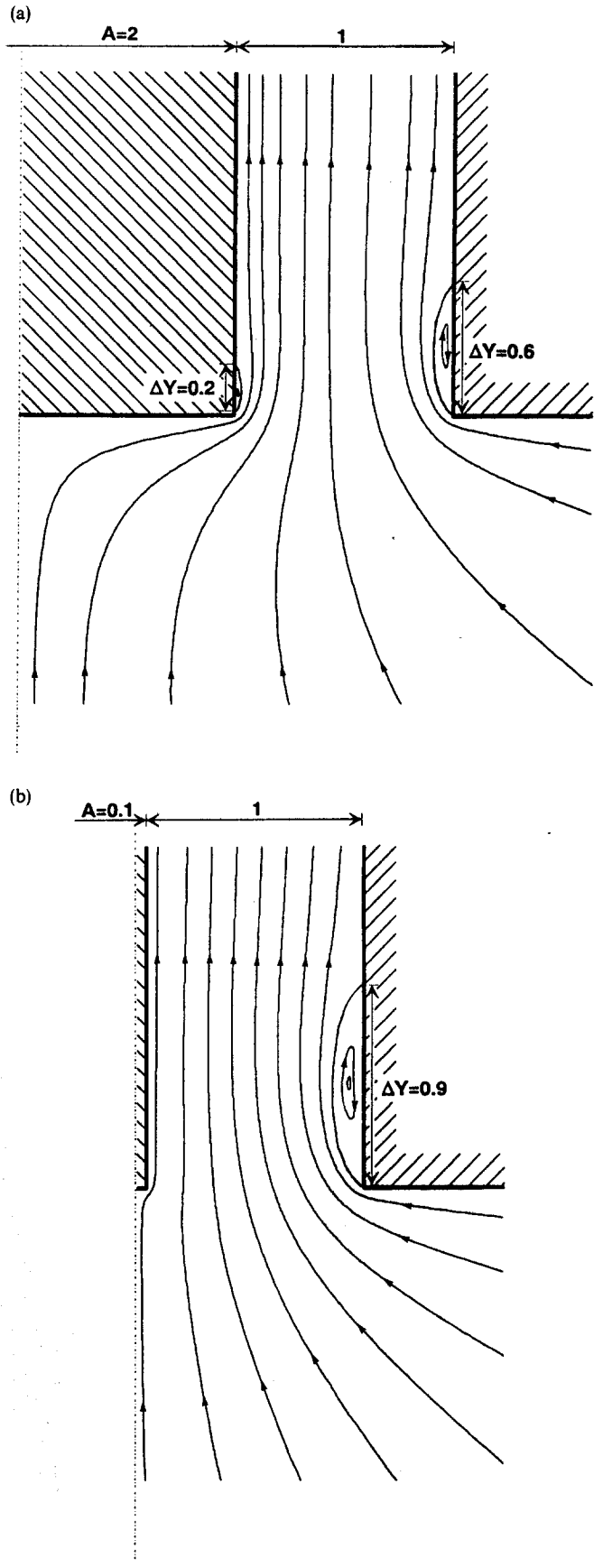

Figure 6 Two-channel system: Streamline pattern in the channel inlet zone: $Gr = 10^5$; $L = 12$; and a) $A = 2$, b) $A = 0.1$

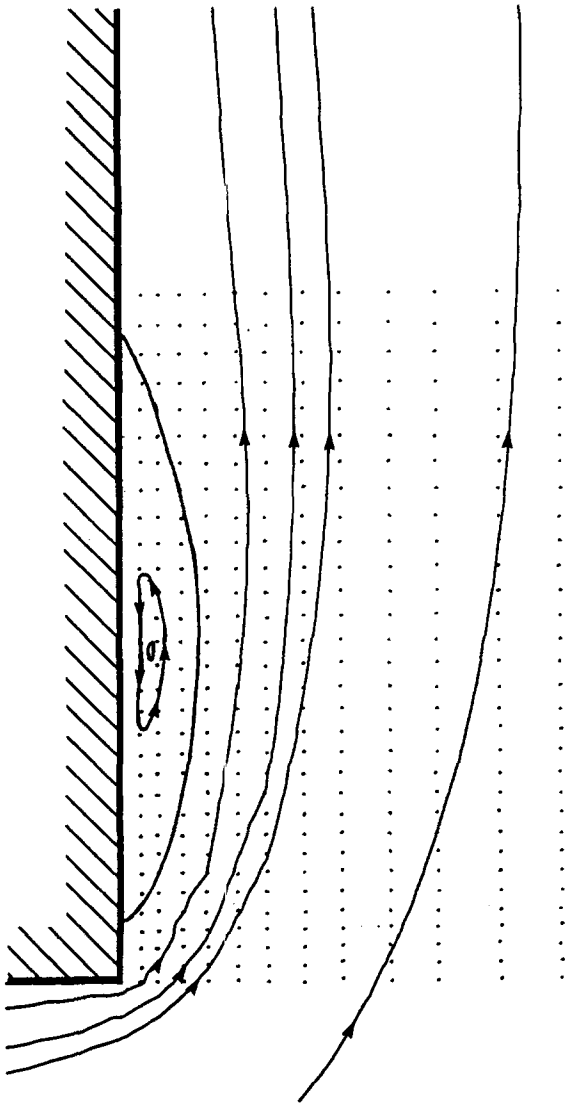

Figure 7 Two-channel system: Mesh density in the flow separation zone on the inner wall: Gr = 10^5; $L = 12$; and $A = 2$

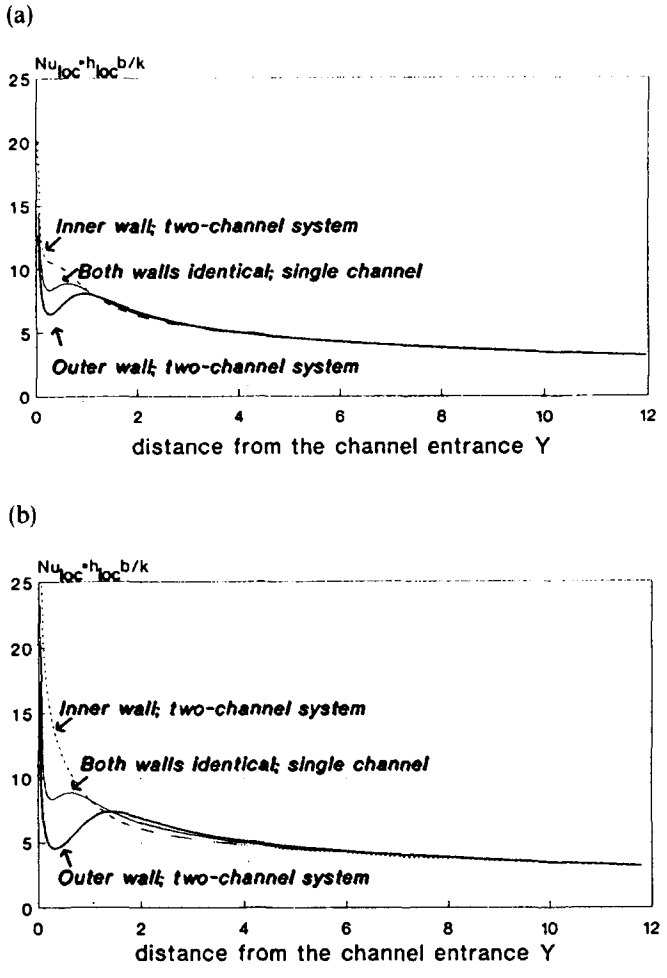

Figure 8 Two-channel system: Distributions of the local Nusselt number along both the inner and outer walls: Gr = 10^5; $L = 12$; a) $A = 2$, b) $A = 0.1$

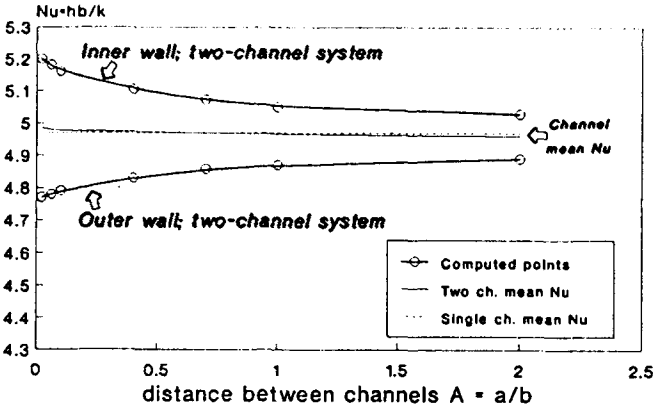

Figure 9 Two-channel system: Mean Nusselt number as a function of the distance A between the channels: Gr = 10^5; $L = 12$

Local Nusselt numbers for the case of flows depicted in Figure 6 are shown in Figure 8. The local heat transfer in the channel entrance region at the inner wall is substantially higher than that at the outer wall. This is because of the large flow separation on the outer wall. Comparison of result for $A = 2$ and $A = 0.1$ shows that bringing the channels closer together increases the difference between the local heat transfer on the inner and outer walls in the channel entrance region. However, sufficiently far from the channel entrance, the effect of interaction diminishes, and each channel behaves as a single one with the local Nusselt numbers almost identical for both walls.

The variation of the mean Nusselt number as a function of distance A between channels for the same values of other parameters (Gr = 10^5, $L = 12$, $R_i = 7$) is shown in Figure 9. The results show that a decrease of distance between the channels increases the mean Nusselt number on the inner wall and decreases it on the outer wall. For the minimum distance studied ($A = 0.02$), heat transfer from the inner wall is roughly 10% higher than that from the outer wall. When compared with a single isolated channel, the heat transfer is higher by 5% and lower by 5% on the inner and outer walls, respectively. When the distance between the channels increases, the effect of interaction decreases (the flow pattern at the channel entrance zone becomes nearly symmetrical), and the heat transfer from both walls approaches that found in a single isolated channel (see dashed curve in Figure 9).

The discussion above shows that the interaction effect is confined to the channel entrance region. To demonstrate properly the magnitude of this effect, we defined the entrance zone as equal to the first 10% of channel length and evaluated heat transfer there. The mean Nusselt number for this zone is smaller by up to 33% on the outer wall and higher by up to 38% on the inner wall, as compared to the case of a single isolated channel.

In shorter channels, the situation is somewhat different. The local Nusselt number distribution for the same parameters as in Figure 8b ($Gr = 10^5$, $A = 0.1$) but for a shorter channel (with $L = 5$) is shown in Figure 10. The induced flow rate is smaller than in the longer channel, the separation bubble has not yet developed, and the resulting changes in the local heat transfer rate caused by the interaction are much smaller. However, the global change in the heat transfer, as measured by percentage of heat transfer in a single isolated channel, is nearly the same as that for the long channel. The reason is that, for the same parameters, the length of the zone where the interaction (and separation) occurs is the same when measured in terms of channel width, regardless of channel length.

When Grashof numbers are small, the induced flow rates are fairly small, and the presence of the second channel has little effect on the flow pattern in the channel entrance region. The flow does not separate, the local heat transfer inside the channel is approximately inversely proportional to the distance from the channel entrance and is the same along both walls. The mean Nusselt number depends little upon the distance between the channels and is almost equal to that of a single isolated channel.

The effect of interaction between the channels can be expressed, regardless of channel length, using a modified Grashof number $\tilde{Gr} = Grb/\ell = Gr/L$ as an independent variable (see Figure 11). It can be seen that the mean Nusselt number increases with an increase of $\tilde{Gr}$, and it is slightly affected by the distance between the channels. The closer the channels are, the higher the difference between the heat transfer from the inner and outer walls.

Correlation

The correlation curve for all data obtained as a part of this study is depicted in Figure 12. The parameter A (distance between the channels) is incorporated using a simple function

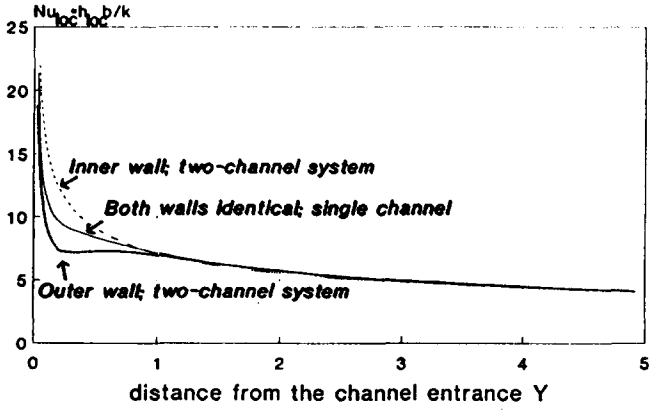

Figure 10 Two-channel system: Distributions of the local Nusselt number along both the inner and outer walls: $Gr = 10^5$; $L = 5$; and $A = 0.1$

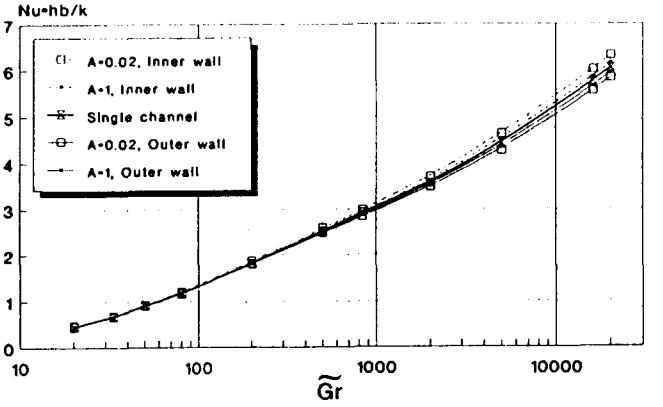

Figure 11 Two-channel system: Mean Nusselt number as a function of the modified Grashof number $\tilde{Gr}$ for various distances A between the channels

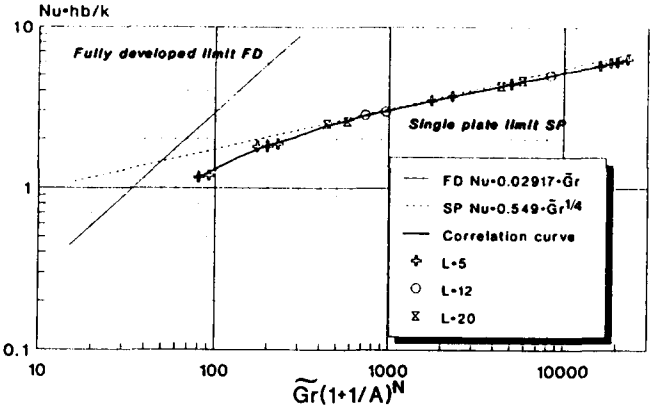

Figure 12 Two-channel system: Correlation curve for the prediction of the mean Nusselt number for the inner and outer walls. Single plate (SP) and fully developed (FD) limits are according to Elenbaas (1942) for a single isolated channel. Exponent $N = +0.035$ for the channel inner wall and $N = +0.035$ for the channel outer wall

in the form $(1 + 1/A)^N$ where the exponent $N = +0.035$ for the inner wall and $N = -0.035$ for the outer wall.

The dependence of the mean Nusselt numbers for both the inner and outer walls in each channel as a function of Gr and A may be expressed, following Churchill and Usagi (1972), as follows:

$$Nu = \left((0.0155Gr)^{-9/5} + \left(0.685 \left(Gr \left(1 + \frac{1}{A} \right)^N \right)^{0.22} \right)^{-9/5} \right)^{-5/9} \tag{6}$$

The equation above is valid for $500 \le \tilde{Gr} \le 20{,}000$; $5 \le L \le 20$; $0.02 \le A \le \infty$, and $Pr = 0.7$ with the accuracy better than $\pm 1.8\%$ and for modified Grashof numbers $100 \le \tilde{Gr} \le 500$ with the accuracy $\pm 5\%$.

Equation 6 can be used for quick evaluation of heat transfer in a single isolated channel ($A \to \infty$), a two-channel system, and for an estimation of the edge effects in a system of more than two channels.

Periodic configuration (infinite number of channels)

Description of the flow geometry

As the number of channels in a system increases, it can be expected that sufficiently far from the edges of the system, the performance of each channel should not be affected by the edge effects. The limiting case corresponds to an infinite number of channels where each channel behaves as a periodic segment. Thus, it is sufficient to analyze only one channel subject to periodic boundary conditions, as shown in Figure 3. Because of symmetry of the flow, the solution domain is reduced further to only half the channel width. Boundary conditions used in this study have the following form (see Figure 3):

Line G–B:

$$U = \partial V/\partial X = \partial T^*/\partial X = 0 \quad \text{for} \quad X = 0, \quad -L_b \le Y \le 0$$

Line B–C:

$$U = V = \partial T^*/\partial Y = 0 \quad \text{for} \quad 0 \le X < 0.5A, \quad Y = 0$$

Line C–D:

$$U = V = 0, \quad T^* = 1 \quad \text{for} \quad X = 0.5A, \quad 0 \le Y \le L$$

Line D–E:

$$\partial U/\partial Y = \partial V/\partial Y = \partial T^*/\partial Y = 0 \quad \text{for} \quad 0.5A \le X < 0.5A + 0.5, \quad Y = L$$

Line E–F:

$$\partial V/\partial X = \partial T^*/\partial X = U = 0 \quad \text{for} \quad X = 0.5A + 0.5, \quad -L_b \le Y \le L$$

Line G–F:

$$U = \partial V/\partial Y = T^* = 0 \quad \text{for} \quad 0 \le X \le 0.5A + 0.5, \quad Y = -L_b$$

The preceding boundary conditions assume that the bottom walls are adiabatic, the vertical walls are isothermal, the flow is fully developed at the exits from the channels, and the flow is uniform and directed upward at a distance L_b below the channels. Distance L_b was determined through numerical experiments, and $L_b = 7$ was found to be sufficient for all calculations. Figure 4b depicts the grid structure corresponding to the channel entrance zone. A grid density guaranteeing accuracy better than 2% for the mean Nusselt number was determined through grid convergence studies similar to those described in detail in the Two-Channel System section. This led to the selection of a 14,275 node grid.

Results

Figure 13a shows streamlines in the channel entrance zone for $Gr = 10^5$, $L = 12$, and $A = 2$. It can be seen that the fluid is unable to turn around the entrance corners without separating. Bringing the channels closer together reduces the amount of turning and suppresses the separation (see Figure 13b). Elimination of flow separation caused by interaction between channels increases heat transfer. This effect can be clearly seen in the distribution of the local Nusselt numbers shown in Figure 14.

The results discussed above differ from those obtained for the two-channel system. In the latter case, decreasing the distance between the channels resulted in a heat transfer increase on the inner wall and a heat transfer decrease on the outer wall (see Figure 9). For periodic channels, heat transfer from both walls is identical and always increases when the distance between channels decreases.

The effect of interaction between the channels can be expressed, regardless of the channel length, using the modified

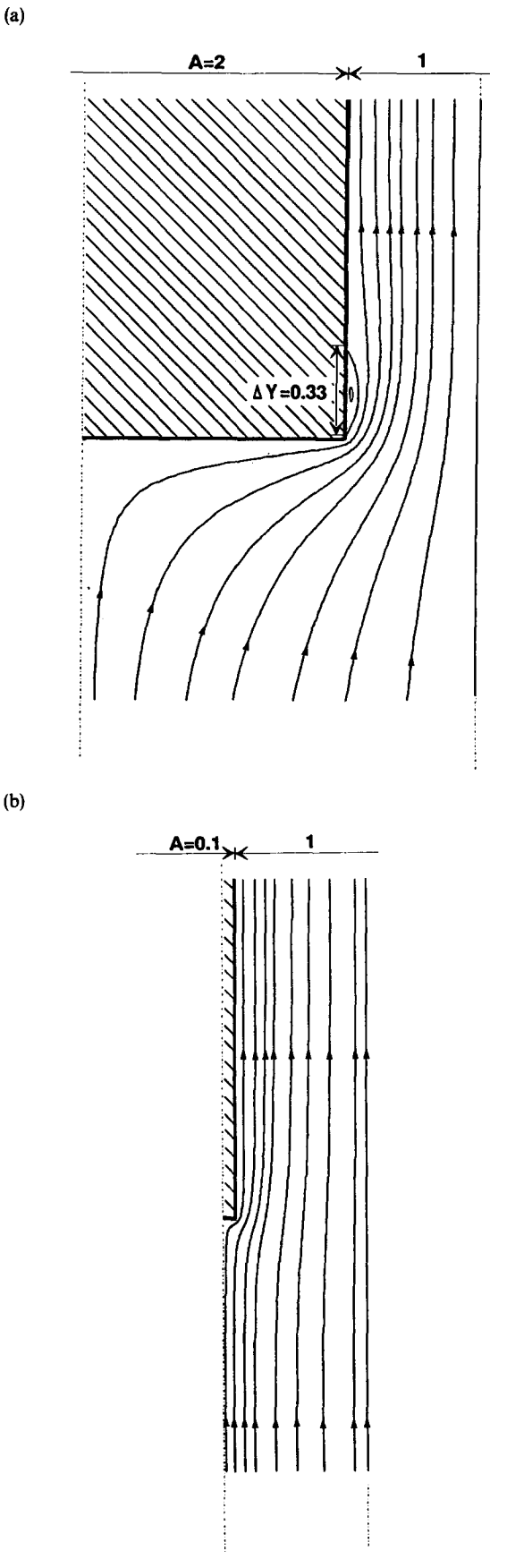

Figure 13 Periodic channel system: Streamlines at the channel entrance zone: $Gr = 10^6$; $L = 12$; a) $A = 2$, b) $A = 0.1$

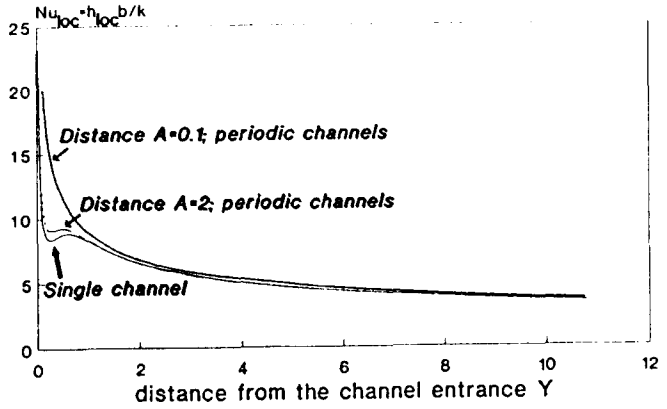

Figure 14 Periodic channel system: Distributions of the local Nusselt number along the channel wall: $Gr = 10^5$; $L = 12$

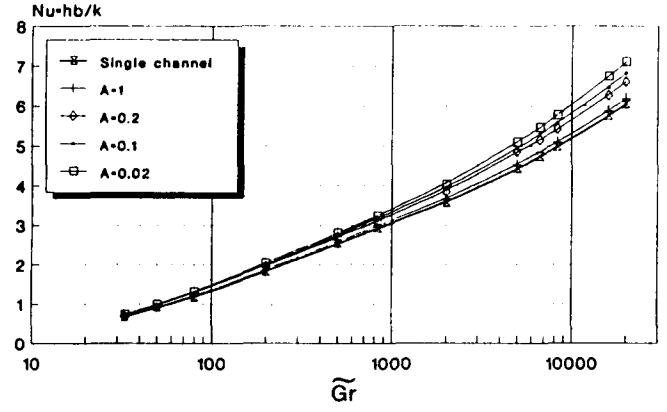

Figure 15 Periodic channel system: Mean Nusselt number for one wall as a function of the modified Grashof number $\tilde{Gr}$, for various distances, A, between the channels

Grashof number $\tilde{Gr}$ as an independent variable. Figure 15 displays the mean Nusselt number as a function of $\tilde{Gr}$ for various distances A between the channels. It can be seen that Nu increases with an increase of $\tilde{Gr}$ and a decrease of A. In the case of channels very close to each other ($A = 0.02$), heat transfer from both walls increases by up to 18%, as compared with a single isolated channel. The interaction between the channels decreases for small $\tilde{Gr}$ and distant channels ($A \geq 1$), and the heat transfer rates approach those found in a single isolated channel. However, we should note that even for very low modified Grashof number but close channels (e.g., $\tilde{Gr} = 50$, $A = 0.02$), the interaction effect still exists, and heat transfer is 10% higher than that found in a single isolated channel.

As already discussed at the beginning of this section, the interaction effect is concentrated in the channel entrance zone. Its magnitude can be properly demonstrated by calculating heat transfer only in the first 10% of the channel length. The corresponding mean Nusselt number was found to increase by up to 48%, as compared to the case of a single isolated channel.

Correlation

Using the methodology suggested by Churchill and Usagi (1972), the following relationships were derived to describe the heat transfer by free convection from wall to heated air inside one of the periodic channels shown in Figure 3:

$$Nu = [(0.019\tilde{Gr})^{-2} + (0.62\tilde{Gr}^{0.23\delta})^{-2}]^{-1/2} \quad (7)$$

where

$$\delta = 0.01[(1.15/A)^{-5/2} + (4.35/A^{0.132})^{-5/2}]^{-2/5} + 1 \quad (8)$$

Equation 7 is valid over the following range of parameters: $200 \leq \tilde{Gr} \leq 20{,}000$; $5 \leq L \leq 20$, $0.02 \leq A \leq \infty$, and $Pr = 0.7$ within an accuracy of $\pm 3\%$. For the modified Grashof number $\tilde{Gr} \geq 2{,}000$. Equation 7 correlate the periodic channel heat transfer with an accuracy better than $\pm 1.2\%$. We should note that Equation 7 does not lead to a universal curve (as was the case with Equation 6), but to a family of curves parameterized by the distance A between the channels.

Discussion

Heat transfer by free convection in parallel vertical channels with isothermal walls was investigated numerically. Results were compared with those describing a single isolated channel. The following conclusions can be made:

(1) In a system of parallel vertical channels the heat transfer in each channel is affected by the presence of a channel nearby.

(2) The interaction between channels increases with an increase of the Grashof number and decreases with an increase of the distance between them.

(3) In a system of periodic channels (infinite number of channels), where no edge effects are present (see Figure 3), heat transfer from both walls in each channel is identical and strongly depends upon the distance between channels. The closer the channels are, the higher is the heat transfer in each channel. When compared with the performance of a single isolated channel, the heat transfer in periodic channels increases by up to 18% because of the interaction with neighboring channels. If only the channel entrance region is considered (e.g., the first 10% of the channel length L), the mean Nusselt number increases by up to 48%.

The results above show that placement of channels closer together significantly enhances heat transfer, primarily in the channel entrance region. This suggests that, from a practical point of view, the electronic components demanding extensive cooling should be placed close to the channel entrance, and the distance between the channels should be minimized.

(4) In a system consisting of two channels, each wall in a channel has a different heat transfer. Heat transfer is enhanced on the channel inner wall (wall closer to the other channel) and reduced on the channel outer wall (wall more distant from the other channel). For very close channels, heat transfer from the inner wall may be up to 10% higher than that from the outer wall. When compared with a single isolated channel, heat transfer in the entrance region (e.g., the first in 10% of the total channel length) of each channel is decreased by up to 33% on the channel outer wall and increased up to 38% on the channel inner wall.

(5) Correlations for mean Nusselt number for both a two-channel system (Equation 6) and a periodic channel (Equation 7) system were obtained. These correlations give an accuracy of $\pm 1.8\%$ for the former and $\pm 1.2\%$ for the latter case.

To check the suitability of the present models to describe heat transfer in a configuration consisting of a finite number of (but more than two) channels, a complimentary study of a three-channel system was conducted using a method similar to that described in the Two-Channel System section. The results

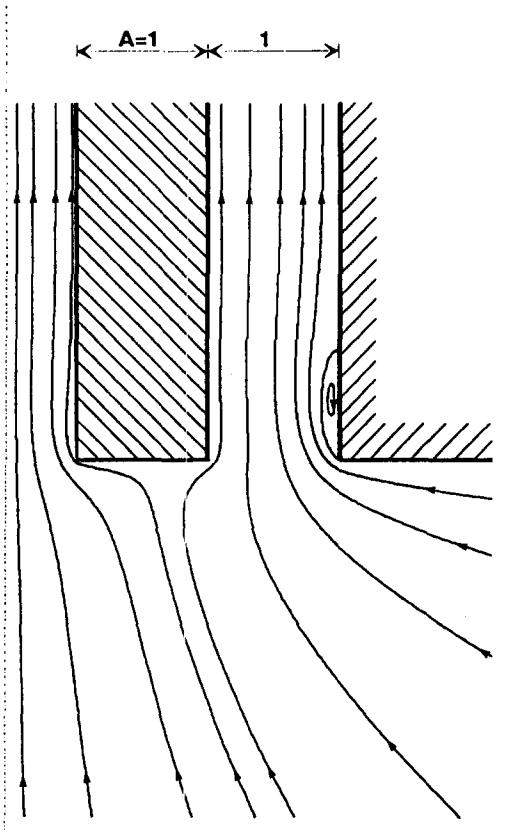

Figure 16 Flow in a three-channel system: $Gr = 10^5$; $L = 12$; $R_i = 10$; and $A = 1$

showed that the heat transfer from both the inner and outer walls of the outer channel is given, with the accuracy better than $\pm 3\%$, using a two-channel model. Heat transfer in the central channel of the three-channel system is still affected by the edge effects and is not accurately described by the periodic model (see Figure 16). The error was found to be approximately 9%.

To determine more accurately the distance from the edges of a system, where the edge effects are negligible, further calculations on more than three channels would be necessary. This has not been done because of the excessive computing resources that would be required. It is expected that with more participating channels, the performance of such a system would tend to that described by the periodic configuration. Consequently, the more channels in a system, the better accuracy provided by correlation (7).

The reader may note that this study suggests that the flow in the channel entrance section may be affected by the shape of the channel bottom corners. Therefore, as a complimentary study, it would be of interest to analyze how different shapes of the channel entrance section affect the heat transfer and the fluid flow at this location.

Acknowledgment

The authors gratefully acknowledge the financial support from NSERC of Canada.

References

Aung, W., Fletcher, L. S. and Sernas, V. 1972. Developing laminar free convection between vertical flat plates with asymmetric heating. *Int. J. Heat Mass Transfer*, **15**, 2293–2308

Bodoia, J. R. and Osterle, J. F. 1962. The development of free convection between heated vertical plates. *J. Heat Transfer*, **84**, 40–44

Churchill, S. W. and Usagi, R. 1972. A general expression for the correlation of rates of transfer and other phenomenon. *AIChE J.*, **18**, 1121–1128

Elenbaas, W. 1942. Heat dissipation of parallel plates by free convection. *Physica*, **9**, 1–28

Kettleborough, C. F. 1972. Transient laminar free convection between heated vertical plates including entrance effects. *Int. J. Heat Mass Transfer*, **15**, 883–896

Kim, S. H., Anand, N. K. and Fletcher, L. S. 1991. Free convection between series of vertical parallel plates with embedded line heat sources. *J. Heat Transfer*, **113**, 108–115

Martin, L., Raithby, G. D. and Yovanowich, M. M. 1991. On the low Rayleigh number asymptote for natural convection through an isothermal, parallel-plate channel. *J. Heat Transfer*, **113**, 899–905

Nakamura, H., Yutaka, A. and Naitou, T. 1982. Heat transfer by free convection between two parallel flat plates. *Num. Heat Transfer*, **5**, 95–106

Naylor, D., Floryan, J. M. and Tarasuk, J. D. 1991. A numerical study of developing free convection between isothermal vertical plates. *J. Heat Transfer*, **113**, 620–626

Naylor, D. and Tarasuk, J. D. 1993a. Natural convective heat transfer in a divided vertical channel: Part I—numerical study. *J. Heat Transfer*, **115**, 377–387

Naylor, D. and Tarasuk, J. D. 1993b. Natural convective heat transfer in a divided vertical channel: Part II—experimental study. *J. Heat Transfer*, **115**, 388–394

Straatman, A. G., Tarasuk, J. D. and Floryan, J. M. 1993. Heat transfer enhancement from a vertical, isothermal channel generated by the chimney effect. *J. Heat Transfer*, **115**, 395–402